Available online at www.sciencedirect.com

ScienceDirect

Scripta Materialia 97 (2015) 5–8

Scripta MATERIALIA

www.elsevier.com/locate/scriptamat

Evolution of dislocation loops in iron under irradiation: The impact of carbon

D. Terentyev[a,*] and I. Martin-Bragado[b]

[a]*Nuclear Materials Science Institute, SCK-CEN, Boeretang 200, B-2400 Mol, Belgium*
[b]*IMDEA Materiales, C/Eric Kandel, 2, Tecnogetafe, 28906 Getafe, Madrid, Spain*

Received 30 August 2014; revised 13 October 2014; accepted 13 October 2014
Available online 4 November 2014

The impact of carbon content on the evolution of dislocation loops in iron–carbon was studied by object kinetic Monte Carlo, explicitly introducing carbon atoms and their atomic features for the first time. We demonstrate that the saturated loop density strongly depends on carbon content and temperature, in good agreement with in situ irradiation microscopy studies. The physical processes responsible for the accumulation and long-range migration of the loops are rationalized with implications for nanostructural evolution in commercial steels upon low-dose-rate neutron irradiation.

Keywords: Iron; Carbon; Dislocations; Radiation; Kinetic Monte Carlo

Modern in situ transmission electron microscopy (TEM) is a powerful tool for gaining an understanding of radiation-induced nanostructural evolution in crystalline materials (e.g. [1,2]). For body-centered cubic iron–carbon (bcc Fe–C) in solid solution, understanding the radiation microstructure is key to assessing the mechanical properties of commercial ferritic nuclear steels under neutron irradiation. Carbon atoms (C) dissolved in an iron/steel matrix occupy octahedral interstitial positions, and are known to strongly interact with point defects (vacancies and self-interstitials) and their clusters (nanovoids and dislocation loops) [1,3,4]. The existence of C–defect interactions leads to a strong impact of C content on the accumulation and recovery of radiation-induced defects, expressed finally in void swelling [5]. Also important, C has a differing affinities for self-interstitial atoms (SIAs), vacancies and dislocation loops (DLs), as revealed by atomistic calculations [6–9]. Unfortunately, direct observation of C atoms and their rearrangement is not possible by in situ TEM, hence the need for supplementary techniques such as a combination of object kinetic Monte Carlo (OKMC) and atomistic methods [10]. The latter approaches have proved that the description of vacancy–carbon annealing in the irradiated Fe–C system is in good agreement with experiments [11].

Treatment of C–SIA and C–DL interactions remains obscure. Previously applied OKMC models for the microstructural evolution in Fe–C and ferritic steels included indirectly the effect of C by imposing ad hoc traps for the DLs or simply by postulating their immobility [10,12,13]. This approach, however, contradicts direct in situ TEM observations reporting one-dimensional (1-D) hopping and coalescence of DLs in bcc Fe [1,14,15] and commercial ferritic steels [15]. Since a general OKMC methodology replicates the well-established model for bcc Fe developed by Domain et al. [12] to address these TEM observations, we employ a novel modular OKMC code (MMonCa), and provide a quantitative assessment of the impact of C on TEM-detectable microstructures under experimentally relevant irradiation conditions.

The open-source MMonCa code is available from Ref. [16] while its technical details and computational advantages are described in Ref. [17]. The most relevant features for the above-formulated goal are: (i) a detailed description of C_N–DL and DL–DL loop interactions, including multiple carbon decoration of DLs; (ii) DLs implemented as 1-D migrating objects, capable of capturing or being trapped by mobile interstitial C atoms; (iii) C atoms being also introduced as objects; and (d) an explicit treatment of C_N–V_M complexes which may grow, dissociate and directly interact with DLs.

Parameterization of the C_N–V_M objects is taken from our recent work [11], based on analysis of ab initio calculations [8]. Strong trapping of SIA clusters by C occurs only for the clusters with ⟨1 1 1⟩ or ⟨1 0 0⟩ orientations, while single ⟨1 1 0⟩ dumbbells and small 3-D migrating SIA clusters do not show any considerable binding with C [9]. Therefore, the effect of carbon is expressed in the trapping by 1-D gliding of $a_0/2\langle 1\,1\,1\rangle$ DLs.

* Corresponding author; e-mail: dterenty@sckcen.be

http://dx.doi.org/10.1016/j.scriptamat.2014.10.021
1359-6462/

The three principal new mechanisms, implemented in the OKMC model, involving the interaction of mobile DLs with C and C–V complexes, are schematically drawn in Figure 1. Following the results of molecular dynamics (MD) and ab initio simulations [10,18], SIA and clusters of up to four vacancies are treated as 3-D migrating objects, parameterized as in Ref. [10]. Larger vacancy clusters are immobile and can only emit vacancies with a dissociation energy, $E_D(V_N - V)$, defined by the sum of the binding, $E_B(V_{N-1} + V)$, and migration, $E_M(V)$, energies of a single vacancy, The key activation parameters describing the mobility and binding of the defects are specified in Table 1, while a full parameterization set is available as online supplementary material.

Consider the upper row in Figure 1: once an SIA cluster has increased to include five atoms, we consider it as an $a_0/2\langle 1\,1\,1\rangle$ loop, with a randomly assigned orientation. The interaction of two intersecting $a_0/2\langle 1\,1\,1\rangle$ loops, consisting of K and N SIAs, results in the formation of an immobile $a_0\langle 1\,0\,0\rangle$ loop on the condition that: (i) their sizes are comparable ($|K-N|/K < 0.1$) and (ii) both K and N exceed 15 defects. Otherwise, both defects coalesce, forming a bigger $a_0/2\langle 1\,1\,1\rangle$ loop. The distinction between these two mechanisms, and the size threshold of 15 SIAs, are applied on the basis of MD simulations and recent self-evolving atomistic MC calculations [19,20]. In the present simulations, $a_0\langle 1\,0\,0\rangle$ interstitial loops are assumed to be immobile because the application of the model is limited to 600 K, where no atomistic or experimental data on the mobility of these loops is available. Finally, the interaction of $a_0\langle 1\,0\,0\rangle$ and $a_0/2\langle 1\,1\,1\rangle$ loops results in a loop with the Burgers vector and properties of the larger loop entering the reaction.

The second row in Figure 1 reflects the interaction of an $a_0/2\langle 1\,1\,1\rangle$ loop (I_K), immobilized by C atom(s), with a mobile V_N cluster (for $N \leqslant 4$). All vacancies are considered to recombine with available SIAs and the resulting configuration will depend on the number of remaining SIAs: for $K-N < 5$, a detached 3-D migrating SIA cluster plus a C atom(s) are formed; otherwise an immobile I_{K-N}–C loop remains.

The third row demonstrates reactions by which multiple trapping of $a_0/2\ \langle 1\,1\,1\rangle$ DLs by C may occur. There are three general possibilities for the DL to combine with C,

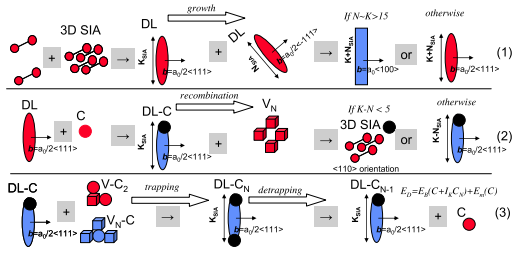

Figure 1. Three principal reaction pathways implemented in the OKMC model. Red objects are mobile, blue are immobile, black circles are interstitial carbon trapped at DLs. Row 1: the growth of $\langle 1\,0\,0\rangle$ and $\langle 1\,1\,1\rangle$ loops by coalescence of SIA clusters; row 2: the trapping of mobile $\langle 1\,1\,1\rangle$ loops by carbon and their further recombination reactions with vacancy defects; row 3: the multiple trapping of $\langle 1\,1\,1\rangle$ loops by C atoms and the emission of C releasing the loop. (For interpretation of the references to colour in this figure legend, the reader is referred to the web version of this article.)

Table 1. Migration (E_m) and binding (E_b) energies of objects introduced in the OKMC model (IM, immobile; DIM, dimensionality of migration).

Defect	E_m (eV)	E_b (eV)	DIM
I1	0.3		3D
I2	0.42	0.8	3D
I3	0.43	I to I_2 0.92	3D
I4	0.43	I to I_3 0.96	3D
I5–I500	0.1	As in Ref. [25] $E_f(I_1) = 3.77$ $E_b(I_2) = 0.8$	1D
V1	0.55		3D
V2	0.54	0.29	3D
V3	0.43	V to V_2 0.37	3D
V4	0.62	V to V_3 0.62	3D
V5–V500		As in Ref. [25] $E_f(V_1) = 2.07$ $E_b(V_2) = 0.29$	IM.
C	0.86		3D
C–V		0.68	IM.
C_2–V	1.1	C to C–V 1.01	3D
C_N–V_M	Taken exactly as in Ref. [11]		
C–I_N ($N \geqslant 5$)		C to I_N	IM.
N = 5–19		0.4	
N = 20–50		0.5	
N = 50–90		0.7	
N = 90–500		0.8	
C_2–I_N ($N \geqslant 5$)		C to C–I_N 0.8	IM.
C_3–I_N ($N \geqslant 5$)		C to C_2–I_N 0.8	IM.

namely by the interaction with: (i) a 3-D migrating C, (ii) a 3-D migrating V–C_2 cluster (proposed to be mobile above 450 K following the analysis shown in Ref. [11]); or (iii) an immobile V_N–C complex. Only the two former paths can result in the multiple trapping of the already immobilized DL–C complex. The binding energy between C and $a_0/2\langle 1\,1\,1\rangle$ DLs, $E_B(I_K\text{–}C)$, varies from 0.4 up to 0.8 eV, depending on the loop sizes, K, and it is ~0.5 eV for 1 nm loops up to 0.7 eV for 2 nm loops. The breakup of the DL–C complex occurs by detachment of the loop consisting of $\langle 1\,1\,1\rangle$ crowdions in the habit plane, as was observed in MD simulations [21]. The addition of one or more C atoms significantly reduces the flexibility of the crowdions and increases the total binding energy of the loop with C atoms. Consequently, the only possible dissociation event for the DL–C_N complex is the successive emission of C atoms, as noted in the third row of Figure 1.

With the above-described mechanisms and parameterization, in situ TEM electron irradiation was modeled to explore the effect of DL–DL interactions and DL–C trapping on the evolution of DL microstructure. To mimic TEM conditions, a KMC sample of $400 \times 200 \times 200 \times a_0^3$ size with $a_0 = 2.87$ A was created, and free surfaces along one direction and periodic boundary conditions along the other two were applied. The free surfaces acted as a sink for radiation-induced defects. The thickness of the KMC box was ~90 nm, close to the typical thickness of a TEM sample zone suitable for providing a reliable estimate of DL densities [2].

The target experimental data [14,22] included the saturated density of DLs in Fe irradiated in the temperature range $T_{irr} = 120$–600 K. In Ref. [14], a sample of 99.999% purity was studied, hence the upper C content was $C_{carb} = 10$ at.ppm. In Ref. [22], a technically pure Fe with controlled C doping of 20 wt.ppm (~100 at.ppm) was used.